Hydrodynamic interactions in hard-sphere suspensions

J.-Z. Xue
Exxon Research and Engineering Company, Annandale, New Jersey 08801
and Department of Physics, Princeton University, Princeton, New Jersey 08544

X.-L. Wu
Department of Physics, University of Pittsburgh, Pittsburgh, Pennsylvania 15260

D.J. Pine
Exxon Research and Engineering Company, Annandale, New Jersey 08801

P.M. Chaikin
Exxon Research and Engineering Company, Annandale, New Jersey 08801
and Department of Physics, Princeton University, Princeton, New Jersey 08544
(Received 3 April 1991)

We study the effects of hydrodynamic interactions on the diffusion of hard spheres in concentrated suspensions. Using a multiple-light-scattering technique, we measure $[H(q)]$, a weighted average of $H(q)$, a function that characterizes the hydrodynamic interaction. By changing the size of the spheres we probe the particle size dependence of $[H(q)]$ and find reasonable agreement with recent calculations for volume fractions $\phi < 0.45$. For large spheres (diameter $2R > 2$ μm), $[H(q)] \rightarrow H(\infty)$ and thus, we measure the short-time self-diffusion coefficient $D_s \equiv D_0 H(\infty)$ where D_0 is the free-particle diffusion coefficient. We find that $H(\infty) = 1 - 1.77(\pm 0.07)\phi$ for $\phi \leq 0.45$. This agrees with the linear (low-concentration) term calculated for short-time self-diffusion. The short-time diffusion coefficient is also found to be continuous across the freezing transition.

PACS number(s): 82.70.Kj, 66.90.+r, 82.70.Dd

I. INTRODUCTION

Particles in colloidal suspensions interact directly through potential interactions and indirectly through a hydrodynamic interaction that is mediated by the surrounding fluid. For many suspensions, the potential interactions are well characterized by the excluded-volume, hard-sphere interaction, which is well understood. By contrast, the hydrodynamic interaction and its concentration dependence is very difficult to accurately determine. Nevertheless, there has been some progress in measuring the concentration dependence of the hydrodynamic interaction through its effect on the self-diffusion coefficient D_s [1–4]. As the particle concentration is increased, the self-diffusion coefficient D_s is reduced by a factor $H(\infty)$ due to the hydrodynamic interaction between particles. That is, $H(\infty) = D_s/D_0 \leq 1$, where D_0 is the Stokes-Einstein free-diffusion coefficient and $H(\infty)$ is a monotonically decreasing function of concentration.

In general, the hydrodynamic interaction depends on correlations between the positions of the colloidal particles. As a consequence, the hydrodynamic interaction is q dependent and is written as $H(q)$ [5, 6]. The q dependence of the hydrodynamic interaction strongly influences the dynamics of concentration fluctuations of a given q. These effects have been studied theoretically by two groups. One group, Beenakker and Mazur [5], extended Batchelor's work [1] on the effects of hydrodynamics on the self-diffusion coefficient. They included many-body interactions to calculate the mobility tensor and then used a generalized Einstein relation to obtain a q-dependent *collective* diffusion coefficient $D_c(q)$ from which they extracted $H(q)$. By contrast, Snook, van Megan, and Tough used an effective-medium theory, and calculated $H(q)$ from an effective two-body mobility tensor [6]. Both theories predict that $H(q)$ is less than 1 for all q and at all concentrations. That is, the hydrodynamic interaction always slows down the relaxation of concentration fluctuations. Furthermore, both theories find that $H(q)$ has a q dependence similar to the static structure factor $S(q)$, thus reflecting the dependence of the hydrodynamic interaction on particle positions. In particular, for $qR \ll 1$, where R is the particle radius, the fast initial relaxation due to the hard-core repulsive potential is partially compensated by the hydrodynamic interaction. For $qR \gg 1$, the relaxation of concentration fluctuations is determined primarily by single-particle motions and $D_c(q)$ approaches the short-time self-diffusion coefficient measured in tracer experiments.

In a previous paper we used a multiple-light-scattering technique known as diffusing-wave spectroscopy (DWS) to probe the concentration-dependent reduction of the diffusion coefficient of a system of model hard spheres due to the hydrodynamic interaction [3]. To extract H(∞) from our measurements, we made extensive use of calculations for the structure factor $S(q)$, the form factor $F(q)$, and models of $h(q)[\equiv H(q)/H(\infty)]$ for a system of hard spheres. In this paper, we relax our reliance on most of these calculations and replace them with experi-

mentally derived quantities. In so doing, we demonstrate that in the limit of large particles, we can directly measure $H(\infty)$ independent of any detailed knowledge about the form of $H(q)$.

II. DWS FOR INTERACTING SPHERES

In the single-scattering case, light is scattered by concentration fluctuations and dynamic light scattering (DLS) measures the cooperative diffusion of the suspended particles [7]. The cooperative-diffusion coefficient $D_c(q)$ is given by the bare Stokes-Einstein diffusion coefficient renormalized by the susceptibility, as given by the static structure factor $S(q)$, and by the hydrodynamic interactions via $H(q)$ [6]:

$$D_c(q) = D_0 \frac{H(q)}{S(q)}. \tag{1}$$

In the short-time limit, the decay of the electric-field autocorrelation function in DLS is given by

$$\langle E(0)E^*(\tau)\rangle \simeq S(q)\exp\left(-q^2 D_0 \tau \frac{H(q)}{S(q)}\right). \tag{2}$$

We can view the multiple-scattering process in an interacting system as a succession of isolated scattering events from correlated regions of spatial extent ξ and separated by the photon mean free path l where, in general, $\xi < l$. Thus, in the strong multiple-scattering limit, photons undergo a random walk in the scattering medium, and the light transport is diffusive [8]. For a large number of scattering events n the contribution to the decay of the autocorrelation function from paths of length $s = nl$ is given by the product of the single-scattering autocorrelation functions, averaged over all angles [3, 4],

$$g_1^s(\tau) = \exp\left(-\left\langle q^2 D_0 \tau \frac{H(q)}{S(q)}\right\rangle n\right). \tag{3}$$

The angular average is weighted by the product of the particle form factor and the structure factor $F(q)S(q)$, i.e.,

$$\left\langle q^2 D_0 \tau \frac{H(q)}{S(q)}\right\rangle = D_0 \tau \frac{\int q^2 \frac{H(q)}{S(q)} F(q)S(q)d\Omega}{\int F(q)S(q)d\Omega}, \tag{4}$$

where $d\Omega$ is the solid angle element. To facilitate the calculation, we express the number of scattering events $n = s/l = (s/l^*) \times (l^*/l)$ in terms of the transport mean free path l^*, which is given by [9]

$$\frac{l^*}{l} = 2k_0^2 \frac{\int F(q)S(q)d\Omega}{\int q^2 F(q)S(q)d\Omega}, \tag{5}$$

where $k_0 = 2\pi/\lambda$ and λ is the wavelength of light in the solvent. For interacting particles, the inverse scattering mean free path is given by

$$l^{-1} = \rho \int_{4\pi} F(q)S(q)\, d\Omega, \tag{6}$$

where ρ is the number density of colloidal particles. The total autocorrelation function $g_1(\tau) = \langle E(0)E^*(\tau)\rangle / \langle |E(0)|^2\rangle$ is obtained by summing the contributions of paths of all lengths, weighted by $P(s)$, and the fraction of paths of length s (determined by the geometry of the sample and the optics). Performing the appropriate averages yields

$$\begin{aligned} g_1(\tau) &= \int P(s) g_1^s(\tau) ds \\ &= \int P(s) \exp\left(-2k_0^2 D_0 \tau \frac{[H(q)]}{[S(q)]} \frac{s}{l^*}\right) ds, \end{aligned} \tag{7}$$

where [] denotes

$$[X(q)] = \frac{\int X(q)F(q)q^2 d\Omega}{\int F(q)q^2 d\Omega}. \tag{8}$$

The photon path length distribution function $P(s)$ can be calculated for a given scattering geometry using the diffusion equation for photons with appropriate boundary conditions [10, 11]. It can be shown that for forward scattering with a broad illumination the autocorrelation function is [10]

$$g_1(\tau) = \frac{(L/\ell^* + \frac{4}{3})\sqrt{x}}{(1+\frac{4}{9}x)\sinh[(L/\ell^*)\sqrt{x}] + \frac{4}{3}\sqrt{x}\cosh[(L/\ell^*)\sqrt{x}]}, \tag{9}$$

where $x = 6k_0^2 D_0 \tau [H(q)]/[S(q)] \equiv 6\tau/\tau_0$. From Eq. (9) we see that one effect of multiple scattering is to speed up the decay of the autocorrelation function by a factor of $\sim (L/\ell^*)^2$. For noninteracting spheres in the dilute limit $x = 6k_0^2 D_0 \tau$. In this case, measurement of the correlation function can directly yield l^*, since D_0 is given by the Stokes-Einstein relation. For interacting spheres, D_0 is replaced by $D_{\text{eff}} \equiv D_0[H(q)]/[S(q)]$. Thus, the diffusion coefficient is again modified by $H(q)/S(q)$, as in the single-scattering limit, but now suitably averaged over all scattering angles because of multiple scattering.

To illustrate the effect of the hydrodynamic interaction on particle diffusion, we calculate numerically the weighted average $[H(q)]$ using the theory of Beenakker and Mazur [5],

$$[H(q)]_{R,k_0,\phi} = \frac{\int_0^{2k_0R} H(qR)_\phi F(qR)(qR)^3 d(qR)}{\int_0^{2k_0R} F(qR)(qR)^3 d(qR)}, \tag{10}$$

which is a function of the particle radius R, the incident wavelength $\lambda = 2\pi/k_0$, and the volume fraction of particles ϕ. In Fig. 1, we show $[H(q)]/H(\infty)$ and $H(\infty)$. It is apparent that for sufficiently large particles, $[H(q)]$ approaches $H(\infty)$. This is largely due to the q^3 weighting in the integration which strongly emphasizes the high-q limit of $H(q)$. For smaller spheres, i.e.,

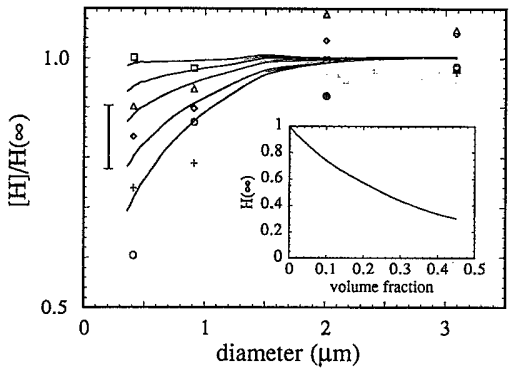

FIG. 1. $[H(q)]$ vs particle diameter at various volume fractions. The symbols are experimental results with $\phi = 0.45$, ○; $\phi = 0.35$, +; $\phi = 0.25$, ◇; $\phi = 0.15$, △; $\phi = 0.05$, □. The solid lines are, from lower curve to upper curve, calculated $[H(q)]$ using theory of Beenakker and Mazur [5] for $\phi = 0.45, 0.35, 0.25, 0.15, 0.05$, respectively. The inset is $H(\infty)$ as a function of the volume fraction calculated from the theory of Beenakker and Mazur. Also shown is a typical error bar for the experimental results.

$2R \leq \lambda$, $[H(q)]$ can be significantly smaller than $H(\infty)$. Note that $[H(q)]_{R,k_0,\phi}$ depends on q and R only through the product qR. Thus, if the wavelength of the incident radiation is held constant, $[H(q)]$ will be a function of R if the hydrodynamic interaction $H(q)$ is indeed a function of q.

From the discussion above, it follows that the ratio $f(R,\phi) \equiv D_0 H(\infty)/D_{\text{eff}} = [S(q)]H(\infty)/[H(q)]$ approaches 1 as the particle size is increased or the volume fraction of the particle is decreased. Using the Percus-Yevick form of $S(q)$ for hard spheres and the Beenakker-Mazur form for $H(q)/H(\infty)$, we find that when the volume fraction ϕ is varied from 0 to 0.45, f changes from 1 to 0.788 for 0.412-μm-diam spheres, from 1 to 0.921 for 0.913-μm-diam spheres, from 1 to 0.991 for 2.01-μm-diam spheres, and from 1 to 0.995 for 3.09-μm-diam spheres. This indicates that if the diameter of the suspending spheres is equal to or greater than ~ 2 μm, the measured value of $[H(q)]$ is within 2% of $H(\infty)$ for all ϕ. Thus, for $2R > 2$ μm, the measured value of D_{eff} is essentially equal to $D_0 H(\infty)$, which is the same as the early time self-diffusion coefficient D_s [12].

III. EXPERIMENT

We employ the DWS technique in the transmission mode in a manner described in Ref. [3]. A laser beam ($\lambda_0 = 488$ nm) was expanded and collimated to uniformly illuminate a 1-cm-diam spot on one side of a cuvette containing the colloidal suspension. In that study we investigated 0.412- and 0.913-μm-diam spheres. In the present work we extend these measurements to 2.01- and 3.09-μm-diam spheres. For these larger spheres sedimentation is a more significant problem, with sedimentation rates ~ 1 cm/day for 2-μm particles. In order to avoid any complications due to sedimentation, we use a 50:50 mixture of H_2O and D_2O as the suspending fluid for the bigger particles. Commercially purchased colloidal suspensions are divided into two portions, and D_2O is added to prepare two samples for each particle size with solvent fluid containing 33% and 67% D_2O, respectively. The samples are then centrifuged and recombined to give a master suspension with $\phi \simeq 0.55$ and with a 50:50 mixture of H_2O and D_2O as the suspension fluid. Portions of the stock suspensions were then diluted using a 50:50 mixture of H_2O and D_2O to prepare a series of samples having volume fractions ranging from 0.03 to 0.55. We added HCl in all samples to give a screening length of approximately 50 Å, thus ensuring that the suspension is well approximated as hard spheres. The volume fractions were determined either by weighing a fraction of each sample before and after drying or by weighing the fractions of the master suspension and suspending fluid used in diluting to proper volume fractions, which are accurate to approximately ± 0.005 and ± 0.01, respectively. The sample temperature was monitored and found to be 22 °C with a fluctuation of about 0.2 °C.

The physical properties of D_2O are slightly different from that of H_2O. At 20 °C, the viscosity of D_2O is 1.23 times greater than that of water; the refractive index at wavelength 5893 Å is 1.3278 for D_2O, compared to 1.3330 for water. In our experiments, the viscosity and the refractive index for the mixture are taken as the volume-fraction average of the quantities for the pure materials. Thus in calculating $D_0 = kT/6\pi\eta R$, we use $\eta = 1.115\eta_0$, with η_0 being the viscosity of water.

For DWS in the transmission mode, light enters an optically thick sample and each photon scatters many times (typically 10^2 to 10^4) before being detected. The characteristic time scale for the autocorrelation function to decay corresponds to the time needed for the path length of a typical photon to change by $\sim \lambda$ due to the motion of the scatterers. Since the decay of the autocorrelation function is due to the aggregate motion of many scatterers, the measurable movement of a single typical particle is much less than the wavelength of light. In our measurements, a typical particle moves less than 50 Å before the autocorrelation function decays. This distance is much less than the mean interparticle spacing so that we always measure the short-time diffusion of the spheres. In our experiments, the thickness of the sample cell was varied from 0.2 to 2 mm for samples having different volume fractions such that the ratio of the sample thickness to transport mean free path L/ℓ^* ranged from 12 to 35 ensuring multiple scattering.

In order to experimentally determine the q-averaged hydrodynamic interaction factor $[H(q)]$, we need to know the transport mean free path l^* of the photons in the medium and the q-averaged static structure factor $[S(q)]$. We use the Percus-Yevick form of $S(q)$ for hard spheres [13] and perform the angular averages numerically to calculate $[S(q)]$. As in Eq. (10) for $[H(q)]$, the angular average $[S(q)]$ corresponds to a $q^3F(q)$ weighting over the interval from 0 to $2k_0R$, and strongly emphasizes the high-q limit where $[S(q)]$ approaches 1. For hard spheres, the peak in $S(q)$ occurs at $qR \approx 3$; in our experiments, $2k_0R$ changes from 7.1 for 0.412-μm diam spheres to 53.3 for 3.09-μm-diam spheres. Thus, in DWS experiments on

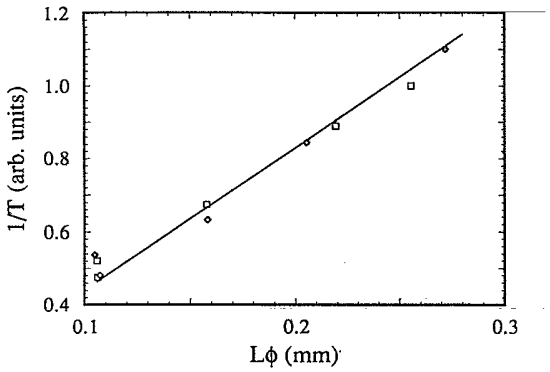

FIG. 2. Inverse transmitted intensity vs $L\phi$. The symbols are from the experimentally measured transmitted intensities: $2R = 3.09$ μm, □; $2R = 2.01$ μm, ◇. The solid line is a fit to Eq. (11) with a reflection coefficient $R = 0.1$ taken from Ref. [14] for the glass-water interface used in our experiments.

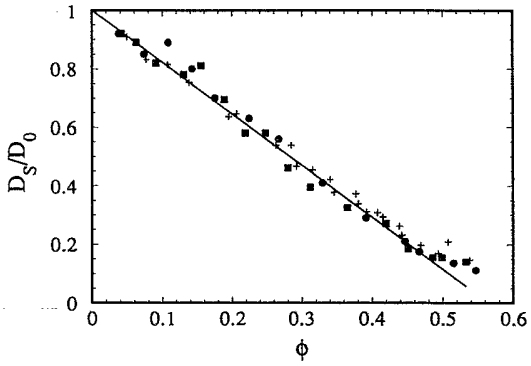

FIG. 3. Measured $H(\infty)$ vs volume fraction for large particles: 2.01 μm (•) and 3.09 μm (■). Also plotted is D_s from Ref. [2] (+). The solid line is a fit to Eq. (12).

large spheres, $[S(q)]$ will be close to 1 and only a weak function of ϕ. In our experiments, $0.565 < [S(q)] < 1.0$ for the 0.412-diam particles and $0.995 < [S(q)] < 1.0$ for the 3.09-diam particles for $0.45 \geq \phi > 0$.

The transport mean free path l^* can, in principle, be measured from the absolute transmitted intensity [14]:

$$T = \frac{\frac{5}{3}(l^*/L)}{1 + \frac{4}{3}[(1+R)/(1-R)](l^*/L)}, \tag{11}$$

where R is a reflection coefficient accounting for the reflection at the water-glass wall interface, and assuming no absorption. In practice, only the relative transmitted intensity is measured, so that some standard with a known value of l^* is needed. The transport mean free path can also be calculated from Eq. (5) using the Mie scattering theory for $F(q)$ and the Percus-Yevick form for $S(q)$. Unfortunately, the Mie theory for the magnitude of $F(q)$ depends very sensitively on variations in the index of refraction of the particles and the solvent. A DWS measurement at low volume fraction provides a convenient absolute calibration for ℓ^*. The dynamic result is typically 5–7 % larger than the calculation. Such differences are often observed and are most likely due to uncertainties in the values of the refractive indices of the solvent and the particles. Therefore, in the following analysis, we use the low-ϕ DWS measurement to normalize the l^* calculated from Mie theory and to provide a reference for the l^* measured using Eq. (11). For large spheres, direct calculation for l^* from Eq. (5) gives $l^* \propto \phi^{-1}$. Thus, from the expression for the transmitted intensity, Eq. (11), $T^{-1} \propto L\phi$. A direct comparison of the measured inverse transmitted intensity versus $L\phi$ is shown in Fig. 2 for 2.01- and 3.09-μm-diam particles. The agreement is excellent. Thus, we have confidence in using the calculated values of l^* for the determination of the hydrodynamic effects.

With the above considerations, $[H(q)]$ and thus D_{eff} can be unambiguously determined by fitting the measured correlation function to Eq. (9) using a nonlinear least-squares fitting routine. In Fig. 3, we plot the measured effective diffusion coefficient D_{eff}/D_0 versus volume fraction for 2.01- and 3.09-μm-diam spheres. We have also plotted the short-time self-diffusion coefficient from a tracer measurement reported by van Megan *et al.* [2]. The data sets are indistinguishable at all volume fractions. Thus, our analysis and experiments show that, for sufficiently large spheres, we can obtain D_s independent of the theoretical model used for $H(q)$. Our data can be fit to the linear form

$$H(\infty) = 1 - 1.77(\pm 0.07)\phi \tag{12}$$

for $\phi \leq 0.45$. To within experimental uncertainty, this agrees with the linear ϕ term calculated by Batchelor [1] who obtains 1.83 and by Felderhof [15] who obtains 1.73.

To show the R dependence of $[H(q)]$ probed in our experiments, we reanalyzed the data from Ref. [3] for 0.412- and 0.913-μm-diam spheres. The results are, along with the results for the large spheres of 2.01 and 3.09 μm, plotted in Fig. 1 at indicated volume fractions for comparison with the theory of Beenakker and Mazur [5]. The data show a clear particle-size dependence which, as expected, is most pronounced for the smallest spheres. To within experimental uncertainty, the theory describes our results satisfactorily for $\phi \leq 0.45$.

As observed in Ref. [3], we again find that D_{eff} varies smoothly as the liquid-solid transition is crossed at $\phi = 0.50$. This continuity of the data across $\phi = 0.50$ illustrates the short-time nature of our measurement. The particles in the crystal move diffusively on a short-time scale and only at longer times feel the strong potential of the surrounding cage of particles which traps them in a single cell of the solid.

In conclusion, we have measured the particle-size dependence of $[H(q)]$, a weighted average of $H(q)$. Our results are consistent with $[H(q)]$ varying with particle size, as expected from the q dependence of $H(q)$. We have also shown that for spheres larger than the wavelength

of light, DWS measures the short-time self-diffusion coefficient of a model hard-sphere system. The ability of DWS to effectively measure the short-time self-diffusion coefficient of a system of spheres follows from the q^3 averaging inherent in the DWS technique which emphasizes the high-q relaxation modes of the system. Our results are in very good agreement with recent calculations and with results obtained in tracer experiments.

ACKNOWLEDGMENT

We thank Dave Weitz for valuable discussions.

[1] G.K. Batchelor, J. Fluid Mech. **74**, 1 (1976); **131**, 155 (1983).
[2] W. van Megan, S.M. Underwood, R.H. Ottewill, N. St. J. Williams, and P.N. Pusey, Faraday Discuss. Chem. Soc. **83**, 47 (1987).
[3] X. Qiu, X.-L. Wu, J.Z. Xue, D.J. Pine, D.A. Weitz, and P.M. Chaikin, Phys. Rev. Lett. **65**, 516 (1990).
[4] S. Fraden and G. Maret, Phys. Rev. Lett. **65**, 512 (1990).
[5] C.W.J. Beenakker and P. Mazur, Physica **120A**, 388 (1983), Physica **126A**, 349 (1984).
[6] I. Snook, W. van Megan, and R. J. A. Tough, J. Chem. Phys. **78**, 5825 (1983).
[7] P.N. Pusey, J. Phys. Math. Gen. **8**, 1433 (1975).
[8] D.J. Pine, D.A. Weitz, J.X. Zhu, and E. Herbolzheimer, J. Phys. (Paris) **51**, 2101 (1990).
[9] P.E. Wolf, G. Maret, E. Akkermans, and R. Maynard, J. Phys. (Paris) **49**, 63 (1988).
[10] D.J. Pine, D.A. Weitz, G. Maret, P.E. Wolf, E. Herbolzheimer, and P.M. Chaikin, *Scattering and Localization of Classical Waves in Random Media*, edited by P. Sheng (World Scientific, Singapore, 1990).
[11] A. Ishimaru, *Wave Propagation and Scattering in Random Media* (Academic, New York, 1978).
[12] We note that we use only the wave-vector dependence of $[H(q)]/H(\infty)$ calculated by Beenakker and Mazur, and not their values of $H(\infty)$, which disagree with the more rigorous low-ϕ theory (Ref. [1]). Since we perform a q average over $H(q)$, and since the effects of $[H(q)]$ tend to counteract those of $[S(q)]$, the values of $f(R,\phi)$ we calculate are insensitive to the exact form of $H(q)$. The calculation of Snook, van Megan, and Tough (Ref. [6]) for $[H(q)]/H(\infty)$ gives essentially the same results.
[13] W. Hess and R.Klein, Adv. Phys. **32**, 173 (1983).
[14] J.X. Zhu, D.J. Pine, and D.A. Weitz (unpublished).
[15] B.U. Felderhof, Physica **89A**, 373 (1977); J. Phys. A **11**, 929 (1978).